UCRL- 92254
PREPRINT

D-T NEUTRON PRODUCTION OF TRITIUM AND ^{4}He IN A LARGE CYLINDER OF ^{6}LiD AND COMPARISON WITH MONTE CARLO CALCULATIONS

Eugene Goldberg, Ronald L. Barber,
Norman A. Bonner, Clyde M. Griffith,
Robert C. Haight, and David R. Nethaway

University of California
Lawrence Livermore National Laboratory
Livermore, CA 94550

This paper was prepared for submittal to
Nuclear Science and Engineering

February 1985

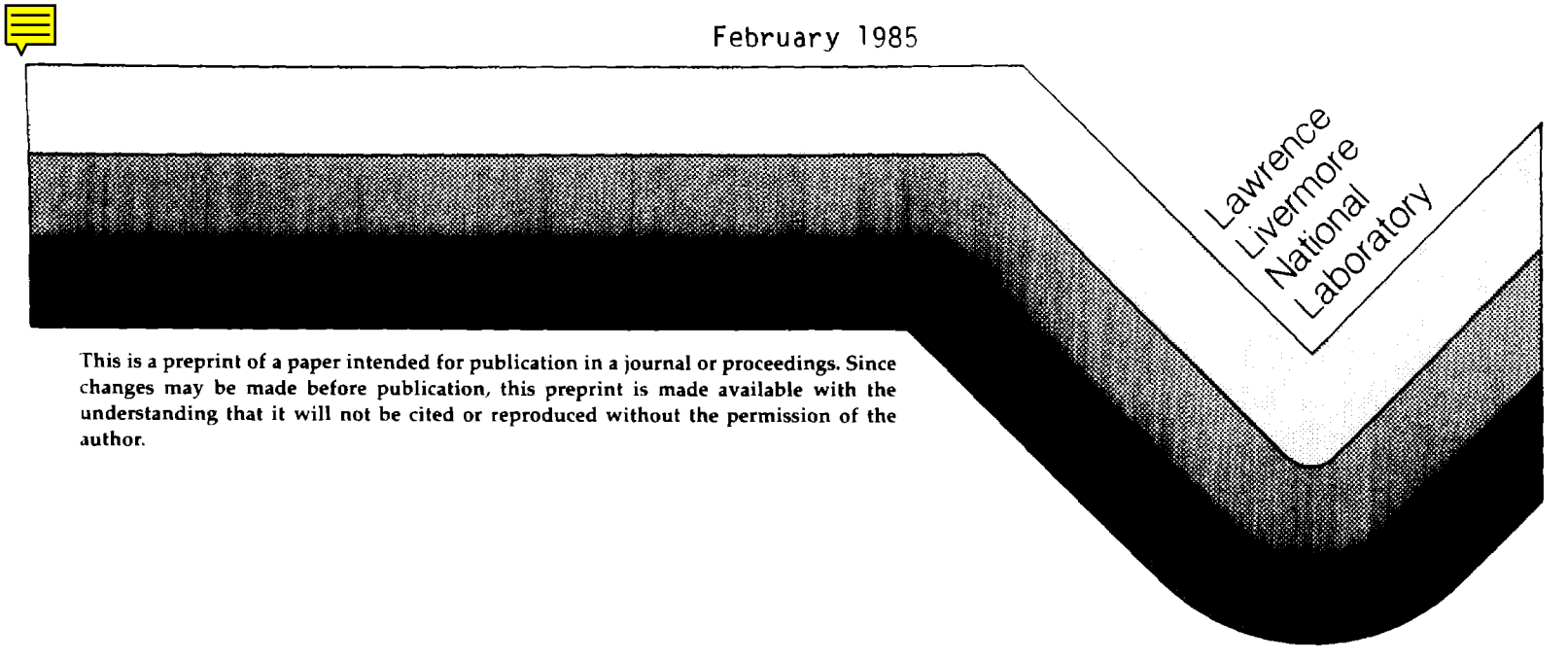

D-T Neutron Production of Tritium and ^{4}He in a Large Cylinder of ^{6}LiD and Comparison with Monte Carlo Calculations

Eugene Goldberg, Ronald L. Barber, Norman A. Bonner,
Clyde M. Griffith, Robert C. Haight, and David R. Nethaway

University of California
Lawrence Livermore National Laboratory
Livermore, CA 94550

Abstract

A large cylindrical assembly of ^{6}LiD was irradiated by a D-T neutron source of high intensity. Samples of ^{6}Li, ^{7}Li, and ^{6}LiH, all contained within Pb, were positioned along the assembly axis and served as targets for ^{4}He and tritium production measurements. The ^{4}He was determined by isotope dilution mass spectrometry while the tritium in the ^{6}LiH wafers was measured by proportional counting of gas samples. Careful comparison to TART Monte Carlo calculations showed excellent agreement. For ^{4}He generation, the experimental values were 1.01 ± 0.06 times that of the calculations, while for tritium the ratio was 1.055 ± 0.07.

Messung von Tritium und ^{4}He Produktion mit D-T Neutronen in einem grossen Zylinder von ^{6}LiD und Vergleich mit Werten berechnet mit Monte Carlo Methoden

Zusammenfassung

Eine grosse zylindrische Anordnung von ^{6}LiD wurde mit einer D-T Neutronenquelle von hoher Intensität bestrahlt. Proben von ^{6}Li, ^{7}Li, und ^{6}LiH, alle in Pb eingeschlossen, wurden entlang der Zylinderachse angebracht und dienten als Targets fuer die Produktion von ^{4}He und Tritium. Das ^{4}He wurde durch Isotopen-Dilution-Mass-Spektrometrie gemessen, während das Tritium in den ^{6}LiH-Scheibchen mittels Proportional-Zählern als Gas gestimmt wurde. Die Resulate waren in guter Übereinstimmung mit Werten berechnet mit TART Monto Carlo Methoden. Für die ^{4}He Produktion wurde das Verhältnis der experimentellen Werte zu den berechneten Werten als 1.01 ± 0.06 ermittelt, für Tritium war das Verhältnis 1.055 ± 0.07.

Production de tritium et de ^{4}He dans un large cylindre de ^{6}LiD sous l'action de neutrons provenant d'une cible de D-T, et comparaison avec des calculs bases sur la methode de Monte Carlo

Resumé

Un large cylindre de ^{6}LiD a été irradié par une source à neutron de D-T située sur son axe, près de sa face anterieure. Des echantillons de ^{6}Li, ^{7}Li et ^{6}LiH, encapsulés dans du plomb, avaient été disposés le long de l'axe et ont été utilisés pour mesurer la production de ^{4}He et de tritium. Le ^{4}He a été mesuré par spectroscopie massique de l'isotope préalablement dilué, tandis que le tritium obtenu dans les pastilles de ^{6}LiH a été detecté par comptage electronique d'echantillons gazeux. Comparaison des measures avec des calculs faits avec le code Monte Carlo TART est excellent. Le rapport des valeurs experimentales et calculées pour l'obtention de ^{4}He est de 1,01 + 0,06, pour le tritium 1,055 + 0,07.

I. Introduction

In the design of a thermonuclear energy generating facility that involves irradiation of lithium-bearing materials with D-T neutrons, one measure of performance is the amount of tritium generated. Another measure, closely related to the energy produced, is the ^{4}He generated, since the major reactions of the breeding cycle are likely to leave ^{4}He as reaction products. Several groups have irradiated large lithium-bearing assemblies to produce tritium,[1-7] the earliest headed by M. E. Wyman who studied tritium buildup in a LiD sphere. The simple geometry generally employed, which anticipates analysis by neutron transport codes is much more appropriate than one which reflects the complexity of an engineering design. A much more stringent test of the validity of the transport code results.

Analysis of one of the more recent integral measurements[4] with the Lawrence Livermore National Laboratory Monte Carlo code, TART,[8] showed that the tritium actually generated exceeded by approximately 9% the TART value. Concern over this discrepancy, and a desire to attempt simultaneous measurements of ^{4}He generation, fostered the present study. Companion experiments[9] were performed in simple geometry, providing opportunities to compare inferred cross sections induced by 15-MeV neutrons to published independent values.

Two runs, spaced three months apart, were performed with a large cylindrical ^{6}LiD assembly. The geometry was essentially two-dimensional, to simplify analysis. Considerable attention was given to the neutron source, the RTNS-I facility of Lawrence Livermore National Laboratory,[10,11] both experimentally and in the code model.[9] The neutron fluence was primarily determined with nuclear activation foils of Nb, Au, Zr, Y, and indirectly, Al, the latter through the reaction, $^{27}Al(n,\alpha)^{24}Na$. Special small capsules

of metallic ^{6}Li or ^{7}Li encased in Pb, and wafers of ^{6}LiH or ^{7}LiH also encased in Pb were accurately positioned along the axis of the large assembly. The capsules were specially designed for mass spectrometric analysis of ^{4}He while the larger wafers were analyzed for tritium content.

II. Experimental Procedure

II. A. Neutron Source Characteristics

An intense neutron source was chosen to give large fluences of neutrons and thereby to enhance the signal-to-background ratios for the measured quantities. The RTNS-I neutron source has been described in detail earlier[10,11] and in a companion paper.[9] A D^{+} beam of 400 keV and 10-20 ma strikes a copper-alloy disc rotating at 1100 rpm which is internally cooled with water. The disc is 1.5 mm thick and the surface struck by the beam is coated with titanium which in turn is loaded with tritium. The rotating target is adjustable in a transverse direction, permitting movement to a fresh band of titanium tritide as the neutron yield drops. The beam spot diameter is nominally 10 mm. Under typical operating conditions, a yield of about 2×10^{12} n/s is realized.

Prior to the integral measurements, the intensity of the neutron field was studied using Al foils positioned at various angles with respect to the beam. The ^{24}Na activity revealed an appreciable dip in the field, about 30% at 90° due to disc scattering of the source neutrons. Reference 9 deals with this topic in detail.

The energy spectrum of the source neutrons was examined in a number of indirect ways. These are (a) neutron yield vs deuteron energy, (b) ratio of induced activity of selected isotopes and in particular $^{90}Zr(n,2n)^{89}Zr$:

$^{27}Al(n,\alpha)^{24}Na$, and (c) the pulse height distribution of $^{29}Si(n,\alpha)^{25}Mg$ events registered in a silicon surface barrier detector. Reference 9 also assesses these techniques.

II. B. Cylindrical ^{6}LiD Assembly

For the sake of brevity, the configuration for only the first integral experiment will be discussed in detail. The two runs had a great deal in common.

Figure 1 illustrates the physical arrangement of components. The ^{6}LiD cylinder, whose nominal diameter and thickness are 900 mm and 500 mm respectively, is in two parts. A cylindrical shroud of ^{6}LiD, 150 mm thick, encircles the source, acting to prevent unnecessary loss of neutrons.

II. B.1. ^{6}LiD Components

The parameters of the ^{6}LiD itself are given in Table I. These three parts are each enclosed in welded stainless steel to prevent attack by water vapor and in addition are coated with a plastic. The outer cylindrical surfaces are covered with 0.81 mm sheeting, the plane surfaces with 0.51 mm sheeting, and the inner surface with a tube of 0.25 mm wall thickness.

Core samples were removed during the drilling of the sample holes in the blocks and densities were measured to be 0.775 and 0.778 Mg/m^3. An average for the blocks is then

$$\rho\ (^{6}LiD) = 0.776 \pm .002\ Mg/m^3$$

with the uncertainty accounting for the spread in measurements. Chemical and isotopic analyses show the ^{6}LiD to be:

$$^{6}Li_{.9564}\ ^{7}Li_{.0444}\ ^{H}_{.0088}\ ^{D}_{.9888}\ ^{O}_{.0016}$$

with a multitude of minor impurities combined in the oxygen fraction.

A foil holder, enlarged in Fig. 1, is interposed between the rotating target and sample hole, along the beam axis, to provide a means of accurate determination of the neutron source location and size. It is nominally 5 cm in length, and the measurements of the activation levels of the foils in comparison to TART calculations provide the axial position of the source to within an uncertainty of 0.5 mm as determined from earlier exercises.

The sample hole, also shown in Fig. 1, is designed to contain 24 samples for ^{4}He measurements, 12 samples for tritium measurements, and otherwise be filled with ^{6}LiD spacers. Au, Y, Zr and Nb foils are located along the sample hole to provide measurements of the shielding character of the assembly but more importantly they enable us to determine the neutron source strength to an accuracy within 5%. The hole of each block is lined with a stainless steel tube of 0.25 mm thickness, as mentioned above, and 26.04 mm I.D. The components of the sample string were assembled in a mylar tube of $\sim$ 0.10 mm thickness and slipped into the hole as a unit.

II.B.2. Contents of Sample Hole

A modular scheme was employed in assembling the sample string. The basic module contained four foils, of Au, Zr, Y, and Nb, followed by a cylindrical wafer of ^{6}LiD with a depression designed to accommodate two Li/Pb capsules for ^{4}He measurement. This "cup" is followed by a cylindrical wafer of

^{6}LiH, encased in Pb, for tritium measurements. The module is nominally 10 mm thick. At greater depths, these modules are separated by ^{6}LiD spacers, each of 10 mm nominal thickness. The ^{6}LiD components are thinly coated with plastic to protect them from attack by water vapor when exposed to air.

II.B.2.a. ^{6}Li/Pb Capsule (^{4}He Measurement)

The design, development, and fabrication of capsules containing lithium for ^{4}He measurement required care so that no ^{4}He escaped and that interfering reactions were kept to a minimum. We settled on a Pb-walled capsule which could be accommodated in the sample hole, and of a mass and shape compatible with the furnace manifold attached to the mass spectrometer at Rockwell International Energy Systems Group (R-I), Canoga Park, California where the ^{4}He analyses were carried out. Initially the active material was to be ^{6}LiD. This we abandoned after a short time upon realization that D_2 would swamp the minute ^{4}He spectrometer signal. We eschewed ^{6}LiH also, anticipating that HD would be confused with the ^{3}He spike. In addition, the hydrogen would have to be gettered, and our samples were anticipated to exceed the gettering capacity of the R-I facility, thus requiring gettering capacity expansion and frequent changes.

The design chosen was exemplified by a ^{6}Li-filled Pb capsule with a nominal 60 mg fill of Li (95.6 atom % ^{6}Li) and 860 mg total mass. The O.D. was 3.81 mm, and nominal length was 17.8 mm. The Pb wall was 0.25 mm thick while the caps were 0.51 mm thick. No voids were allowed in the capsule. The cylindrical slug of Li metal was sealed under vacuum to avoid inclusion of trace amounts of He expected to be in the drybox atmosphere.

The Pb was chosen for a number of reasons. First, the ^{4}He-production cross-section at $E_n \sim$ 15 MeV as measured by Kneff[12] of R-I is very small - 0.62 mb - and so would not contribute a measurable fraction of ^{4}He upon

vaporization. Secondly, ^4He is very insoluble in Pb at room temperatures and so Pb is a good seal and should insure containment of ^4He. Further, the Pb is easily melted and vaporized in the R-I furnace. Also, because Pb is so soft, fabrication of the capsule and sealing were expected, and were found to be, relatively trouble-free.

After some unsuccessful attempts to speed development, we evolved the following procedure which was found to produce a product whose baseline (i.e. unexposed to neutrons) ^4He content as determined by R-I measurements and prototypes was $\sim 2 \times 10^{10}$ atoms of ^4He.

Starting with Pb stock which was 99.99% pure, the metal was first melted for at least 18 hrs at 520°C under vacuum to drive off any ^4He. The material was then rolled to a thickness of 2.0 mm and circular discs about 10 mm in diameter were punched out and placed in an extrusion press which produced a tube of 0.25 mm wall thickness sealed at one end. The excess Pb was left as a flared cone and, before removal, the tube was vacuum tested for pinholes and flaws using the flared portion as a gasket. The tube was cut to length and also its closed end was shaped to match the shape of the ^6Li slug which was to slip in. Caps of Pb 0.51 mm thick were fabricated from the vacuum-melted stock. The tube and cap were weighed.

The ^6Li metal was also vacuum melted, here for 24 hours at 670°C. Extrusion of a strand of 3.18 mm diameter followed. This was then sheared in a special cutting assembly to a length of 16.8 cm, and weighed.

The ^6Li slug was inserted into the vertical tube and gently settled to the tube bottom. The cap was placed in the tube over the ^6Li, the tube lip was then bent gently inward with a simple tool to clamp the lid in place and finally the unit was placed in a press. The tube was evacuated prior to sealing, and then 172 MPa gage (25000 psi) was briefly applied while the tube

was evacuated. The excess Pb flowed locally to seal the capsule. Upon removal the capsule was weighed to verify that all material was accounted for, after which any Pb which was loosely connected to the capsule was trimmed away.

After fabrication, the capsule was immersed in anhydrous ethyl alcohol. If any Li was exposed, bubbles emanated from the Li sites. Only those capsules which were free of bubbles were accepted. The procedure outlined tends to limit possible leak sites to the cap area, and so the inspection was made with a stage microscope, concentrating on the capped end.

II.B.2.b. ^{6}LiH/Pb Wafer (Tritium Measurement)

For tritium measurement, ^{6}LiH wafers were covered overall by Pb foils 0.25 mm thick to produce samples of 3.5 mm thickness and 25.4 mm diameter. The details of fabrication and the wafer performance were discussed in Ref. 9. For both ^{6}LiH and ^{7}LiH wafers, the nominal hydride mass was 1.0 g.

Possible tritium loss is less of an issue for these wafers than for ^{4}He loss from the Li/Pb capsules because the hydrogen of the ^{6}LiH acts as a carrier for the tritium and loss of a significant portion of tritium would be signaled by a corresponding loss of hydrogen. The measurement is in units of atoms of tritium per atom of hydrogen which is quite satisfactory for our purpose. The Pb coating is perhaps to be valued more as a seal against attack by water vapor than as a tritium barrier.

II.B.2.c. Placement of Sample Tube Components

Table II lists the components of the sample tube for the first run. The cups, wafers, and spacers were of very uniform quality, and within each group,

the masses were within one percent of the mean, while ^{7}Li masses were bunched tighter. The average characteristics (-used to develop the modular parameters for TART) are:

Foils; thickness (mm):

Au:	#1-17	(.051)
Nb:	#2-5	(.079)
Nb:	#1,6-17	(.137)
Zr:	#5	(.127)
Zr:	#6-17	(.114)
Ni:	#2-5	(.025)
Y:	#6-17	(.145)

Capsules:

^{6}Li, isotopic purity 95.5%
Li mass: .06054 g
Pb mass: .9171 g

^{7}Li, isotopic purity 99.99%
Li mass: .0699 g
Pb mass: .8852 g

Pb:
Tube: Pb mass: .840 g
Sheet: Pb mass: .185 g
Wire: Pb mass: .184 g

^{6}LiD cups, isotopic purity: 95.6% ^{6}Li

Mass: 1.752 g
Thickness: 6.303 mm
Depth of trough: 4.043 mm

Wafers, isotopic purity: 95.6% ^{6}Li

Mass: .9678 g ^{6}LiH (95.6% ^{6}Li)
3.8378 g Pb
Thickness: 3.503 mm

^{6}LiD spacers, isotopic purity: 95.6% ^{6}Li

Mass: 3.9461 g
Thickness: 10.00 mm

The axial spacing between the frontal face of the leading Au foil and frontal face of the ^{6}LiD of the large assembly (where the sample hole begins) was 45.4 mm. The stainless steel sheet pressed against the face was 0.51 mm thick.

All components slipped into a mylar tube of 25.4 mm I.D. and 0.10 mm thickness. The cups' diameters were slightly undersize while the wafers and spacers fit snuggly in the tube. The disparity was taken into account in the calculations.

The capsule pairs were wrapped in .025 mm thick Pb sheets to insure that no ^{4}He made in adjacent materials could become imbedded in the capsule walls. We also emplaced segments of Pb wire alongside the capsules to provide additional means to assess ^{4}He production in Pb but chose not to analyze them because they were redundant with the empty lead capsules.

The assembled sample tube was inserted from the rear. After careful alignment the sample tube entered easily. The procedure for placement of the ^{6}LiD assembly consisted first of the determination of source position by irradiating a copper foil and subsequent autoradiography. The assembly, with the sample tube removed, was positioned so that the image of cross hairs (beamed from a distant downstream station along the beam pipe axis) was visible on the target surface at a position in accord with the autoradiograph. Further, the ^{6}LiD cylinder face was located nominally 5 cm from the target outer surface and the distance was measured for later specification in the Monte Carlo calculations. Finally the sample tube was inserted with a 1.0 mm shim between the target outer surface and upstream face of the sample tube. The shim was removed prior to the irradiation. This 1.0 mm spacing was expected to represent only approximately the gap during the run, because of (a) deformation of the target during rotation, (b)

inaccuracies of the measurement due to poor visibility (we used a mirror), or (c) possibly different spacings for the different bands on the target. We believe these uncertainties add up to no more than 0.5 mm. We must depend upon interpretation of the activation foils for a more accurate determination of location of the sample tube contents with respect to the source spot.

III. TART Calculation for Run 1

Figure 2 illustrates the geometry of a key TART problem which modelled the first run. Sixty-seven minutes of Cray-I time were consumed for 4×10^6 particles in the calculation which involved 150 spatial zones. We did not employ particle weighting for the study of the first run. The statistical uncertainty of the Monte Carlo calculations of ^{4}He and tritium production was kept within the accuracy of the measurements. The same model for the source (i.e. multi-angle, multi-energy) used in Ref. 9 was used here.

To reduce the statistical noise of the TART calculations of ^{4}He and tritium generated within the respective small zones, parallel problems considerably simplified and with large zones were run to get the shape of the tritium and ^{4}He generation curves. These were used to guide us in developing a smooth curve through the points generated in the detailed TART calculation. The ratios of experimental to calculated ^{4}He and tritium did refer the experimental values to the smooth curve representing calculations. We believe the comparison to be improved by such a procedure.

To avoid the tedium of specifying each component explicitly in the TART calculations, modular descriptions were constructed with care so that axial positions were altered by no more than ± 0.15%. Masses were generally honored to within 1% since components such as the ^{6}LiD spacers were very uniformly manufactured.

IV. Experimental Results for Run 1

IV.A. Neutron Source Characteristics

IV.A.1. Source Spectrum and Size

On the day prior to start of the prolonged run, we sought to characterize the source by a few of the techniques discussed above. First we shifted to a relatively fresh band and with the ^{6}LiD assembly far removed from the target area generated a Neutron Yield vs E_D curve. We found, in contrast to the correlation of Ref. 9, a neutron yield which agreed within 10% with the fresh target yield of Seagrave (assuming TiT)[13] or our newly generated curve (assuming $TiT_{1.5}$).[9,14] This result suggests a uniform tritium loading and therefore value for $\bar{E}_n$ of 14.98 MeV in the forward direction.

Following this, while the assembly was still removed, we observed the pulse height distribution (p.h.d.) of the silicon surface barrier detector at $\theta = 96°$, for calibration of the energy scale and determination of the detector resolution. Then we moved the detector to 180° and used the $^{29}Si(n,\alpha_0)$ peak to indicate the average energy of the source neutrons as in Ref. 9. The average neutron energy was found to be constant within 50 keV over the course of the irradiation.

After the 47 hour run was completed, the Au and Nb foils closest to the neutron source were autoradiographed to determine the shape, size, and transverse location of the source. We found the spot to be $\sim$ 10 mm in diameter and centered with respect to the activation foils at the face of the sample tube to within 1 mm, up-down as well as sideways. Consequently, the source disc was assigned a 5 mm radius and was centered on the cylinder axis in the TART calculations.

IV.A.2. Source Strength

The neutron source intensity averaged approximately 1.8×10^{12} n/sec over the length of the irradiation. An accurate value for the strength was inferred from the four families of activation foils accurately located within the sample tube. These are of Au, Nb, Zr, and Y. The few Ni foils in the forward region were not utilized because of lack of confidence in their cross sections. Since the ^{6}LiD assembly influences the activation values significantly, especially at greater depths of penetration into the ^{6}LiD, this process of inferring source strength involves careful reference to the TART calculations.

A pair of proton recoil counters, which viewed the neutron source from an upstream station at a distance of 1.00 m, was also employed. These are meant to act as absolutely calibrated flux monitors for the bare source. However, in the present situation, the massive ^{6}LiD assembly reflects neutrons back to these counters. An experiment showed the enhancement factor to be 1.11. A TART calculation gave a factor of 1.17. This discrepancy could be due to the counter bias setting procedure. Where the counter data are used in the following analysis, the experimental enhancement factor will be honored.

Figure 3 illustrates the Z^2 x (product atoms/g of activation foil) for the four sets of foils employed, with (Z) measured from the source plane. We selected a gap of 0.65 mm between the rotating target outer surface and frontal surface of the leading Au foil for reasons to be discussed below. The statistical accuracy of the counts per foil was generally ± 1%. Each set follows a smooth curve. The Au and Nb sets are less attenuated than the Zr and Y sets since the latter have distinctly higher reaction thresholds [all

(n,2n)] than the former. TART calculations were run to determine the source strength accurately. The TART-generated function:

$$\psi = Z^2 \times (\text{atoms of radioactive product/g of foil})/\text{source neutron}$$

was seen to be not very sensitive to the choice of gap size between target and leading gold foil. Since we display in Fig. 3 the directly measured (Z^2 x atoms/g), the corresponding quantity is (ψ x S) so the source strength is simply a multiplier. The excellent quality of the data encourages us to seek a match to greater depths of ^{6}LiD - and indeed we see in general very good agreement between slopes for all four sets out to values of Z = 200 mm. By choosing a gap of 0.65 mm (which, when added to the 1.52 mm thickness of the backing of the rotating target, is equivalent to an axial spacing of 2.17 mm between the source plane and frontal face of the leading Au foil) we achieve fairly good fits for the measurements with Z>5 cm in the cases of Nb and Au.

The Au and Nb foils closest to the source were first counted and then small 3.2 mm diameter discs were punched from each foil central region and counted. The source model in TART is a circular disc which generates neutrons uniformly, and is clearly an idealization. Also the measured activity of the small discs is extremely sensitive to the source-disc spacing. By discounting the closest data point and insisting on good fits for the other data points, we find for the Nb foils (Z < 200 mm) a source strength of 2.98×10^{17}n with a standard deviation of 1% of the mean.

The ^{93}Nb(n,2n)^{92m}Nb cross sections used by TART were a special set drawn from a compilation supplied by Nethaway.[15] A small additional adjustment upward of 0.5% was incorporated to account for the difference in

the reference $^{27}Al(n,\alpha)^{24}Na$ cross sections between Nethaway (who measured the Nb cross section relative to the Al value) and Tagesen and Vonach's more recent evaluation.[16]

From the $^{197}Au(n,2n)^{196}Au$ data we infer a source strength of 2.94 $\pm$ 0.10 x 10^{17}n using the findings of Ref. 15 corrected by 0.5% as we did above. We used here the TART cross section set corrected by a multiplier based on an average over the Seagrave spectrum of 2.11 b for the TART set and 2.16 b for the set recommended by Nethaway.[15] The fit as a function of depth was not as good as in the case of Nb, suggesting the possibility that the cross section for Au is not accurately portrayed away from the high energy peak.

The $^{90}Zr(n,2n)^{89}Zr$ cross section has also been carefully measured with respect to the $^{27}Al(n,\alpha)^{24}Na$ reaction.[17] The cross sections inputted to TART produced values which were then adjusted by 0.4% to account for the modest difference with Pavlik's findings. The isotope fraction for ^{90}Zr is taken at 0.515. A source strength of 3.03 $\pm$ .05 x 10^{17}n was found.

The Y set by similar calculations led to a source strength of 2.94 x 10^{17}n. In spite of the fact that fewer foils were exposed, this value is in excellent agreement with the source strength determined from the other activation foils.

We are also able to estimate the source strength from the proton recoil counter data. Using the reflection correction of 1.11 arrived at experimentally, we find a source strength of 3.06 x 10^{17}n. A grand average, with all five values equally weighted, is 2.99 x 10^{17}n.

We choose finally a source value:

$$S = (2.99 \pm .09) \times 10^{17} n$$

with the ± 3% uncertainty reflecting statistical and estimated systematic uncertainties.

IV.B. Tritium in ^{6}LiH

Eleven of the twelve ^{6}LiH wafers in the sample tube provided acceptable data. The ^{6}LiH wafers (95.5% ^{6}Li) employed in the overall study came from a common stock so many background samples could be intercompared. The tritium was specified in units of [atoms tritium/liter H_2(STP)], since the wafer material is decomposed in the analytic process. The measurement accuracy has been specified at 2%, after intercalibration with an NBS standard sample.[9] The average background value, from five samples, is $4.9 \pm 1.5 \times 10^{10}$ atoms tritium/liter H_2(STP). On the average, each wafer released 1.53 liters H_2(STP) upon decomposition.

Table III lists the experimental values of tritium released for each capsule. We see the background to be a very small fraction of the measured values - even for the deepest wafer, the background is only ∿ 8% of the gross measurement. The uncertainty in the background, only ∿ 2.4% of that signal, is more relevant to the error analysis. Figure 4 illustrates the findings.

IV.C. ^{4}He in ^{6}Li and ^{7}Li

Table IV summarizes the ^{4}He findings of the first RTNS-I run. The capsules at the deepest positions (Z > 23 cm) were not analyzed because the

background capsules from that batch registered excessively high ^{4}He levels. The batch which included all the others was limited in number. Their background, taken at 7.6 x 10^9 atoms per capsule, was based on one reading plus the trend at that time among the capsules tested during development. Figure 5 illustrates the experimental results for the ^{6}Li capsules. The deterioration of quality at greater depths is evident.

An accuracy of 2% is attached to the mass spectrometeric analysis of the ^{4}He by the R-I group, based on detailed attention to the calibration of the detector and many years of experience.[12,18] The smooth behavior of the experimental points in Fig. 5 suggests that additional contributions to the spread about the correct values are generally modest.

V. Experimental Results for Run 2

The second run, planned from the outset, served well to demonstrate the reproducibility of the data. Quality control, particularly regarding the Li capsules used for ^{4}He measurements, was a potential problem, and intercomparison of data from the two runs helped greatly to expose spurious readings.

The second run was the more ambitious of the two. We sought additionally to expose ^{7}LiH wafers in the sample hole and to expose ^{6}Li capsules and ^{6}LiH wafers at greater depths. Five ^{7}Li capsules were exposed. Activation foils were emplaced more deeply as well. The second run was of 66 hour duration, and the target was fresh at the outset. The silicon surface barrier detector demonstrated that the average neutron energy varied within 50 keV of its starting value, expected to be E_n = 14.98 MeV.

The best fit of TART-generated foil activation values to experiment was achieved with a gap of 1.40 mm between the outer surface of the source disc

and frontal face of the leading gold foil (implying an axial spacing between source plane and Au frontal face of 2.92 mm). Prior to the run, the gap was measured to be 1.1 mm. For this run, the axial distance between the frontal faces of the leading Au foil and ^{6}LiD of the assembly was 41.4 mm, which was 4.0 mm shorter than in the first run. The fluence determined by recoil counters was assigned a 5% uncertainty. The calibration was modified by the count enhancement factor of 1.11 described above. Utilizing the data from the Au, Nb, Zr and Y foils as well as the proton recoil counters, the source strength was found to be

$$S = 4.99 \pm 0.20 \times 10^{17} \text{ n}$$

with $\bar{E}_n$ = 14.98 MeV and a spectrum as given by Seagrave (see Ref. 9 for a discussion of the applicability of this spectrum).

Figure 6 illustrates the activation foil data for the second run, assuming a 1.4 mm gap. The data is presented as $(\Delta Z)^2$ x (Activity) to highlight the attenuation of the ^{6}LiD. The quality of the data is quite high revealing exponential dropoffs of activity at greater depths.

The ^{4}He and tritium measurements will not be listed explicitly here for brevity. However the findings will be included when comparison is made to TART calculations. We note that the ^{4}He backgrounds per capsule for the batches used in the second run were for ^{6}Li : $9.2 \pm 4.6 \times 10^{10}$ atoms and for ^{7}Li: $8 \pm 8 \times 10^{10}$ atoms. At the shallowest station the ^{6}Li capsule registered 550×10^{10} atoms ^{4}He while the ^{7}Li capsule registered 262×10^{10} atoms ^{4}He.

The tritium background correction for the ^{6}LiH was more modest: $4.9 \pm 1.5 \times 10^{10}$ atoms T/liter H_2(STP). The shallowest wafer registered 1418 x

10^{10} atoms T/liter H_2. A few outlying points suggesting contamination levels of 4 x 10^{12} atoms T/liter will be apparent in a later illustration.

The tritium background for the ^{7}LiH wafers was found to be excessively high. Isotopic analysis showed the ^{7}LiH to contain deuterium in variable quantities, that is $^7Li^2H$. The deuterium is generally accompanied by tritium in the isotopic enrichment process as in this case. We therefore could not derive values for the tritium production values for ^{7}Li from this experiment.

VI. Comparison to TART Monte Carlo Calculations

The TART code calculates, per source neutron, the tritium or ^{4}He per zone assigned to the actual wafer or capsule. A convenient quantity to evaluate which lends itself to the intercomparison of the two runs is the ratio of product generated in the experiment to that in the calculation as a function of distance of detector from the source. For example, the ^{6}Li capsule ratio for ^{4}He generation is:

$$R_\alpha = \frac{(\text{atoms } ^4\text{He per capsule})_{exp}}{S(\text{atoms per capsule per neutron})_{TART}}$$

where the denominator contains the source strength inferred experimentally and the TART value for ^{4}He taken from the smoothed curve through the calculated points discussed earlier.

VI.A. Tritium in ^{6}LiH Wafers

^{6}LiH wafers at shallow stations require special attention since the neutron spectrum there is relatively undegraded, and such neutrons are relatively ineffective as tritium generators. The companion study[9]

in which ^{6}LiH wafers were directly exposed to 15 MeV neutrons compelled us to examine in detail the effects of various perturbations which were not initially included in the TART calculations. These included D-D neutrons from deuterium buildup in the target and beam collimator scattering. Their influence quickly subsided as deeper wafers were considered. TART calculations were performed for the more important issues. We found, for example, that tritium production was enhanced by 9 ± 4% for the shallowest ^{6}LiH wafer when all these effects were included. The D-D correction, 4%, was the largest, and the collimator correction, 2%, was next. At the next station, the enhancement dropped to 6 ± 3%.

One mechanisim which introduces tritium into the wafer but which was not present in the experiment of Ref. 9 involves recoil of tritons created in adjacent ^{6}LiD capsule cups and spacers. These items were painted with a thin (.025 mm) plastic coat to prevent attack by water vapor. Since the tritons arising from the $^{6}Li(n,T)\alpha$ reaction generally have a range in ^{6}LiD or CH_2 at room temperature of about 6 mg/cm^2, a calculation shows that the wafer tritium content would be enhanced by 0.5% at most. We therefore discount this correction.

Figure 7 summarizes the tritium results for the two integral measurements. Three outliers occurred in the second run. The data from the first run did not exhibit any anomalies out to a distance of 340 mm, or about 300 mm into the ^{6}LiD. No ratios of experimental to calculated tritium generated are below a value of 1.01. If the three outliers are discounted, the average ratio, weighted according to the local specific tritium production, is:

$$\left(\overline{\frac{\text{Exp.}}{\text{Calc.}}}\right)_{\text{Tritium in } {}^{6}LiH} = 1.055 \pm 0.07$$

The uncertainty is a summation by quadrature of the uncertainties from the components participating in the determination of the ratios. The major contributor, except at large depths, is the source strength uncertainty, estimated at ± 3% for the first run and ± 4% for the second. Beyond a spacing of 300 mm, Monte Carlo statistics are the major contributor for the first run. The ratio is seen to be within one standard deviation of unity.

VI.B.1. ^{4}He in Li/Pb Capsules

Figure 8 summarizes the findings of ^{4}He generated in the ^{6}Li capsules for the two runs. Recall that the data has shown a peaking in Z^2 x ^{4}He per capsule at Z ∿ 180 mm. At shallower distances we see the ratio of experiment to calculation to be generally within 5% of unity. At larger distances, outliers are evident.

The group of points at Δ Z ∿ 210 mm shows a clear disparity between the two runs - the points from the second run hover near unity while those from the first run are well beyond 2 S.D. of the later data. The error bars represent the cumulative uncertainty in ^{4}He measurements, and Monte Carlo statistics. In this case, heavier weight should be given the points from the second run, because we have a much more detailed understanding of the ^{4}He content of the background capsules than we have of that of the June run.

Our capsules were fabricated following a procedure which sought to reduce the ^{4}He content to less than 5 x 10^{10} atoms per capsule. We employed a vacuum melt procedure, monitoring the ^{4}He as it was released. Apparently this procedure does not provide a uniform product. One possible explanation may be gleaned from recent materials studies motivated by questions relevant to controlled fusion reactor design. Evidence has accrued[19] of clustering of helium atoms in the host medium which hinders escape of the helium. Our

procedure which saw the ^{6}Li heated under vacuum at 670°C for 24 hr apparently was not adequate to generate a uniform helium-free product. Judging from the variation among background samples, the residual helium after the vacuum melt is markedly nonuniform throughout the lithium.

Monte Carlo calculations show that at a distance of 200 mm from the source, the tritium generated in ^{6}Li is about 60% of the ^{4}He generation, and the ratio rises to 72% at greater depths. If, then, the tritium outliers signal a real peak, the ^{4}He data should manifest a peak at the same Z, and vice versa. Coincidence does not appear to occur, strengthening our inclination to discount the outliers.

When this is done, a straightforward average of the ^{4}He ratio of experiment to calculation, weighed by the axial profile (i.e. Fig. 8), results in:

$$\overline{(Exp./Calc.)}_{^{4}He \text{ in } ^{6}Li} = 1.01 \pm 0.06$$

We may then conclude that the current TART Monte Carlo model with its present set of neutron cross-sections is in close agreement with the integral experiments discussed here, insofar as ^{4}He generation in ^{6}Li is at issue.

VI.B.2. ^{4}He in ^{7}Li/Pb Capsules

Four ^{7}Li capsules were successfully exposed in the first integral measurement and five in the second. Background capsules were respectively one and two in number. No buildup, as in the case of ^{6}Li, was anticipated, so the capsules were positioned at relatively shallow depths. For the deepest capsule, in the second run, ΔZ (source-capsule center distance) was 183 mm, and the uncertainty in background was 32% of the gross signal.

The quality of the data at very shallow positions appear to be

satisfactory, where the signal is due primarily to neutrons relatively undegraded in energy. We may extract a cross section value at E_n = 15 MeV, if we assume the relative dependence of cross section with energy is correct in the TART calculation. For the forward capsule station, TART calculations show a $\sim$ 6% enhancement in ^{4}He production in ^{7}Li due to the ^{6}LiD assembly. If we weight the cross section values by (^{4}He gross)^2, we find:

First integral exp't.: $\sigma_7(n,x\alpha) \simeq 301$ mb (E_n = 15 MeV)

Second integral exp't: $\simeq 317$ mb (E_n = 15 MeV)

8-4-83 (free-in-air): $\simeq 336$ mb (E_n = 15 MeV)

The last entry, to be discussed in a separate paper, was of higher quality than the first two. If, again, we weight the cross sections inferred from individual capsules from the three runs, we find:

$$\sigma_7(n,x\alpha) = 329 \text{ mb} \pm 16 \text{ mb} \quad (E_n = 15 \text{ MeV})$$

where the uncertainty represents the spread among the measurements.

VI.C. ENDF/B-V.2. Cross Sections

The TART code utilizes a cross section library which has been developed at LLNL.[20] To facilitate comparison to the more popular ENDF set, the latest version being ENDF/B-V.2[21], TART calculations were repeated with the ENDF/B-V.2 cross sections for ^{6}Li, ^{7}Li, and D. First a simple representation of the ^{6}LiD cylindrical assembly was employed and then we used a point source in a large ^{6}LiD sphere, big enough to insure no leakage.

The results were quite similar. For an infinite medium of ^{6}LiD (95.5% ^{6}Li, 4.5% ^{7}Li), and E_n = 14.1 MeV, the ENDL set of Sept. 18, 1984 gave 1.26 tritons per neutron and 2.01 ^{4}He atoms per neutron. The ENDF/B-V.2 set

gave 1.27 and 2.01, respectively. We see excellent agreement here. For the simple representation of the ^{6}LiD assembly, the (ENDF/B-V.2/ENDL) tritium and ^{4}He ratios are plotted on Figs. 7 and 8. In the case of tritium production, we see that the ENDF/B-V.2 set leads to 1-2% more tritium than the ENDL set, an amount well within experimental uncertainty. For ^{4}He production, the two sets agree well except at shallow depths. A likely explanation is based on the difference in cross sections for the ^{6}Li(n,n'd)α reaction, with ENDF/B-V.2 values lower than those of the ENDL set. The role of this reaction becomes subordinate to the ^{6}Li(n,t)α reaction as greater depths are attained.

VII. Summary

We have simultaneously generated within a ^{6}LiD cylindrical assembly tritium in samples of ^{6}LiH and ^{4}He in samples of ^{6}Li and ^{7}Li metal, by bombardment with D-T neutrons. Two separate and similar runs were performed. The tritium and ^{4}He measurements were carefully compared with TART Monte Carlo calculations. Special efforts were expended to keep overall uncertainties below 8%. The major contributor was that associated with the neutron source strength determination, which relied primarily on four families of activation foils, all threshold detectors.

We found that TART predictions agreed well with the experiments. If we weight the measurements made along the ^{6}LiD axis according to (tritium/g ^{6}Li), we find:

$$\overline{(T_{exp.}/T_{calc.})}_{^{6}LiH} = 1.055 \pm 0.07$$

- Within experimental error, TART agrees with the experimental findings.

The ^{4}He experimental findings are also in good agreement with TART. For ^{4}He in ^{6}Li capsules, after weighting according to $(^{4}He/g^{6}Li)$, we find:

$$\overline{\left(^{4}He_{exp}/^{4}He_{calc}\right)_{^{6}Li}} = 1.01 \pm 0.06$$

The ^{7}Li results were of poorer quality, in large measure because of the relatively rapid dropoff of ^{4}He generated per capsule as greater depths into the ^{6}LiD were attained.

TART calculations were also done with ENDF/B-V.2 cross sections. For the ^{6}LiD assembly geometry, we found that the ENDF/B-V.2 set leads to 1-2% more tritium than ENDL, while the ^{4}He generation is unchanged except at very shallow depths. Here, because the $^{6}Li(n,n'd)\alpha$ set in ENDF/B-V.2 is smaller than the ENDL set, the ratio is 0.9 at the ^{6}LiD surface, rising rapidly to unity at a depth of 70 mm. Therefore, the ENDF/B-V.2 set leads to 1% less ^{4}He than the ENDL set.

Acknowledgments

We are grateful to E. W. Burke for his sustained interest and support throughout the study. Many others contributed significantly, with good cheer, in the development and fabrication of detectors and major hardware. E. F. Plechaty and J. R. Kimlinger helped to make our use of TART a friendly experience. We thank also I. D. Proctor and the operating and maintenance staff for the virtually trouble-free performance of the RTNS-I facility through out the activity. D. W. Kneff and B. M. Oliver of Rockwell International Energy Systems Group were very responsive in their careful analyses of the ^{4}He-bearing capsules, easing our burdens through the development phase. We are indebted to V. C. Rupert and R. W. Bauer for translations of the abstract. This work was performed under the auspices of the U.S. Department of Energy by the Lawrence Livermore National Laboratory under contract number W-7405-ENG-48.

References

1. M. E. Wyman, "An Integral Experiment to Measure the Tritium Production from ^{7}Li by 14 MeV Neutrons in a Lithium Deuteride Sphere," LA-2234, Rev., Los Alamos Scientific Laboratory (1972).
2. R. Herzing, L. Kuvjpers, P. Cloth, D. Filges, R. Hecker, and N. Kirch, Nucl. Sci. Eng., 60, 169 (1976).
3. H. Bachmann, J. Fritscher, F. W. Kappler, D. Rusch, H. Werle, and H. W. Wiese, Nucl. Sci. Eng., 67, 74 (1978).
4. A. Hemmindinger, C. E. Ragan, and J. M. Wallace, Nucl. Sci. Eng., 70, 274 (1979).
5. H. Maekawa, K. Tsuda, T. Iguchi, Y. Ikeda, Y. Oyama, T. Fukumoto, Y. Seki, and T. Nakamura, "Measurements of Tritium Production-Rate Distribution in Simulated Blanket Assemblies at FNS," NEACRP-L-268, Department of Reactor Engineering, Tokai Research Establishment, JAERI (1983).
6. P. Cloth, D. Filges, H. Geiser, R. Herzing, G. L. Stocklin and R. Wolfle, Proc. 8th Symposium on Fusion Technology, Noorwijkerhowt, The Netherlands, 17-21 June 1974.
7. P. W. Benjamin, H. Goodfellow, J. Gray, J. W. Weale, Measurements of Neutron Reaction Rates Produced by a 14 MeV Neutron Source at the Centre of a Cylindrical Lithium Pile, AWRE Report No. NR 4/64, Aldermaston, Berks, 1964.
8. E. F. Plechaty and J. R. Kimlinger, "TARTNP Coupled Neutron-Photon Monte Carlo Transport Code," UCRL 50400, Vol. 14, Lawrence Livermore Laboratory (1975).

9. E. Goldberg, R. L. Barber, P. E. Barry, N. A. Bonner, J. E. Fontanilla, C. M. Griffith, R. C. Haight, D. R. Nethaway, and G. B. Hudson, to be published.

10. R. Booth, J. C. Davis, C. L. Hanson, J. L. Held, C. M. Logan, J. E. Osher, R. A. Nickerson, B. A. Pohl and B. J. Schumacher, Nucl. Instrum. Methods 145, 25 (1977).

11. R. Booth and H. H. Barschall, Nucl. Instrum. Methods 99, 1 (1972).

12. D. W. Kneff, B. M. Oliver, H. Farrar IV, L. R. Greenwood, and F. M. Mann, submitted for publication in Nucl. Sci. Eng.

13. J. D. Seagrave, "D(D,n)^{3}He and T(D,n)^{4}He Neutron Source Handbook," LAMS-2162, Los Alamos National Laboratory (1958).

14. J. H. Ormrod, Nucl. Instrum. Methods 95, 49 (1971); see also H. H. Anderson and J. F. Ziegler, "Hydrogen Stopping Powers and Ranges in All Elements," Vol. 3 of The Stopping and Ranges of Ions in Matter, organized by J. F. Ziegler, New York: Pergammon (1977).

15. D. R. Nethaway, Private Communication (1983); see also D. R. Nethaway, Nucl. Phys. A190, 635 (1972), and J. Inorg. Nucl. Chem. 40, 1285 (1978).

16. S. Tagesen and H. Vonach, Physics Data 13-3, Karlsruhe (1981).

17. A. Pavlik, G. Winkler, H. Vonach, A. Paulsen and H. Liskien, J. Phys. G: Nucl. Phys. 8, 1283 (1982).

18. H. Farrar IV, W. N. McElroy, and E. P. Lippincott, Nucl. Technol. 25, 305 (1975).

19. G. J. Thomas, W. A. Swansiger, and M. I. Baskes, J. Appl. Phys. 50, 6942 (1979); see also C. L. Bisson and W. D. Wilson, Proceedings, Tritium Technology in Fission, Fusion and Isotopic Applications, Dayton, Ohio, Apr. 29-May 1, 1980, American Nuclear Society National Topical Meeting.

20. R. J. Howerton, R. E. Dye and S. T. Perkins, "Evaluated Nuclear Data Library," UCRL 50400, Vol. 4, Rev. 1, Lawrence Livermore National Laboratory (1981); cross section set used was TL831128.

21. ENDF/B-V2, ^{6}Li(Mat 1303, Mod 1), evaluated by G. Hale, L. Stewart and P. G. Young, Los Alamos National Laboratory (1977); also, ENDF/B-V2, ^{7}Li(Mat 1397, Mod 1), evaluated by P. G. Young, Los Alamos National Laboratory (1983); also, ENDF/B-V, D(Mat 1302), evaluated by L. Stewart, Los Alamos National Laboratory and A. Horsley, Aldermaston Laboratory (1978).

Table I

Parameters of the ^{6}LiD Assembly Components

Item	I.D. (mm)	O.D. (mm)	Thickness (mm)	Mass (kg)	Density (Mg/m^3)
Shroud	460.25	901.22	149.9	54.40	0.770
Block 1	26.67	901.57	248.9	122.90	0.774
Block 2	26.64	900.94	247.9	122.56	0.776

Table II. Contents of Sample Tube, First Run

Station	Foils (Diameter, mm)	Capsule Cup	Wafer	Spacer (mm)	Measured Position[a] (mm)
1	Au, Nb (25.4)	-	-	-	0.00
2	Au, Nb, Ni (12.7)	-	-	-	6.46
3	Au, Nb, Ni (")	-	-	-	16.73
4	Au, Nb, Ni (")	-	-	-	27.06
5	Au, Nb, Ni, Zr (12.7)	-	-	-	37.44
6	Au, Zr, Y, Nb (25.4)	^{6}Li, ^{7}Li	^{6}LiH	-	48.86
7	Au, Zr, Y, Nb (")	^{6}Li, Pb	^{6}LiH	-	59.34
8	Au, Zr, Y, Nb (")	^{6}Li, ^{7}Li	^{6}LiH	^{6}LiD (10)	70.01
9	Au, Zr, Y, Nb (")	^{6}Li, Pb	^{6}LiH	^{6}LiD (")	90.59
10	Au, Zr, Y, Nb (")	^{6}Li, ^{7}Li	^{6}LiH	^{6}LiD (")	110.98
11	Au, Zr, Y, Nb (")	^{6}Li, Pb	^{6}LiH	^{6}LiD (")	131.50
12	Au, Zr, Y, Nb (")	^{6}Li, ^{6}Li	^{6}LiH	^{6}LiD (")	152.11
13	Au, Zr, Y, Nb (")	^{6}Li, ^{7}Li	^{6}LiH	^{6}LiD (20)	172.89
14	Au, Zr, Y, Nb (")	^{6}Li, ^{6}Li	^{6}LiH	^{6}LiD (")	203.53
15	Au, Zr, Y, Nb (")	^{6}Li, ^{6}Li	^{6}LiH	^{6}LiD (30)	233.96
16	Au, Zr, Y, Nb (")	^{6}Li, ^{6}Li	^{6}LiH	^{6}LiD (40)	274.59
17	Au, Zr, Y, Nb (")	^{6}Li, Pb	^{6}LiH	^{6}Li (220)	325.06

a. Relative to station 1.

Table III

Summary of Tritium Measurements in ^{6}LiH Wafers Exposed in First RTNS-I Run

Station No.	$(\Delta Z)^a$ (mm)	T/liter H_2 x 10^{-12}	$(T-B)(\Delta Z)^2$ x 10^{-14}
6	59.8	8.21	2.92
7	70.4	7.70	3.79
8	81.0	7.27	4.73
9	101.5	6.17	6.30
10	122.1	5.63	8.32
11	142.7	4.25	8.55
12	163.2	- [d]	-
13	183.8	2.84	9.44
14	214.3	2.08	9.31
15	244.9	1.61	9.37
16	285.5	1.03	7.96
17	336.0	0.65	6.75

[a] Distance from source to center of wafer.
[b] Tritium atoms per liter H_2(STP).
[c] Tritium atoms $\cdot$ mm^2 $\cdot$ (liter H_2)$^{-1}$; B = background, $4.9 \pm 1.5 \times 10^{10}$ atoms tritium per liter H_2(STP).
[d] Rejected because of sample fractionation.

Table IV

^4He Measurements in ^6Li and ^7Li Capsules for Run 1

at RTNS-I, S = 2.98×10^{17}n

Capsule No.			Li Mass (mg)		ΔZ^a (mm)	$^4He^b \times 10^{-10}$		$(\Delta Z)^2 \times (^4He - B)^c \times 10^{-12}$	
^6Li	^7Li	Pb	^6Li	^7Li		^6Li	^7Li	^6Li	^7Li
9	11		60.9	70.1	53.8	344	164	98.7	46.9
11		A	61.0		64.4	256		105	
10	12		62.0	70.5	74.9	216	93.7	118	51.2
12		B	60.3		95.5	150		137	
13	13		62.3	69.5	116.1	111	32.9	144	42.1
14		C	60.8		136.6	85.0		157	
6			60.1		157.2	66.0		163	
7			59.5		157.2	65.3		162	
5	14		59.4	69.7	177.7	51.4	11.6	162	31.1
4			59.7		208.3	51.2		222	
1			59.9		208.3	71.3		278	

[a] Distance from source to center of capsule
[b] Atoms of ^4He per capsule
[c] Backgrounds; ^6Li: 7.6×10^9; ^7Li: 1.8×10^{10}; Pb A, B: 4.7×10^9 each; Pb C was not measured.

Figure 1. Physical arrangement of the experiment. Details are shown of the components within the sample hole and also of the activation foil holder and contents protruding from the sample holder.

Figure 2. TART Monte Carlo geometric representation of ^{6}LiD assembly and rotating target assembly for the first run.

Figure 3. Measured and calculated activities of Zr, Y, Nb, and Au foils as a function of axial distance from source plane for first run. For the calculated values, $S = 2.98 \times 10^{17}$ n is used. The function, $(Z)^2$ x (atoms of product/gm of sample) vs Z illustrates the attenuation due to the ^{6}LiD clearly.

Figure 4. Measured and calculated tritium generated per liter of hydrogen as a function of axial distance for the first run. The source strength is taken to be 2.99×10^{17} n. The line represents findings from an idealized TART calculation with fine statistics.

Figure 5. Measured and calculated ^{4}He generated per ^{6}Li capsule as a function of axial distance for first run. Also included is a line inferred from a TART calculation with simpler geometry and better statistics. The source strength is taken to be 2.99×10^{17} n.

Figure 6. Measured and calculated activities of Zr, Y, Nb, and Au foils as a function of axial distance from source plane for the second run. $S = 4.99 \times 10^{17}$ n is used in the determination of the calculated points.

Figure 7. Ratio of experimentally determined tritium generated per wafer of ^{6}LiH to calculated values. Findings from Runs 1 and 2 are illustrated. Uncertainties represent total of contributions from experiment and calculation. See text for explanation of solid line.

Figure 8. Ratio of experimentally determined ^{4}He generated per capsule to calculated values. Findings from Runs 1 and 2 are shown. The cumulative uncertainties are illustrated.

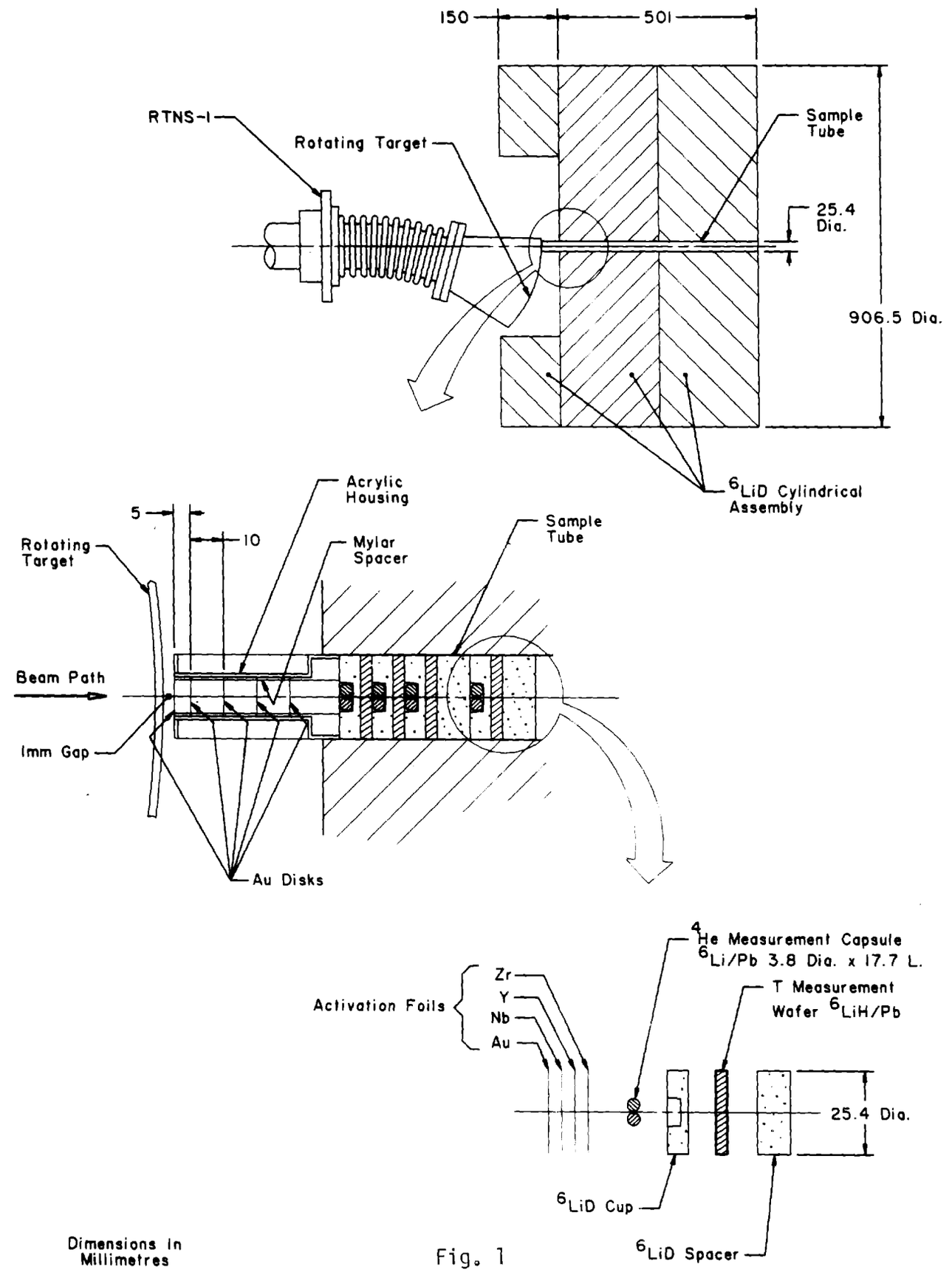

Dimensions In Millimetres

Fig. 1

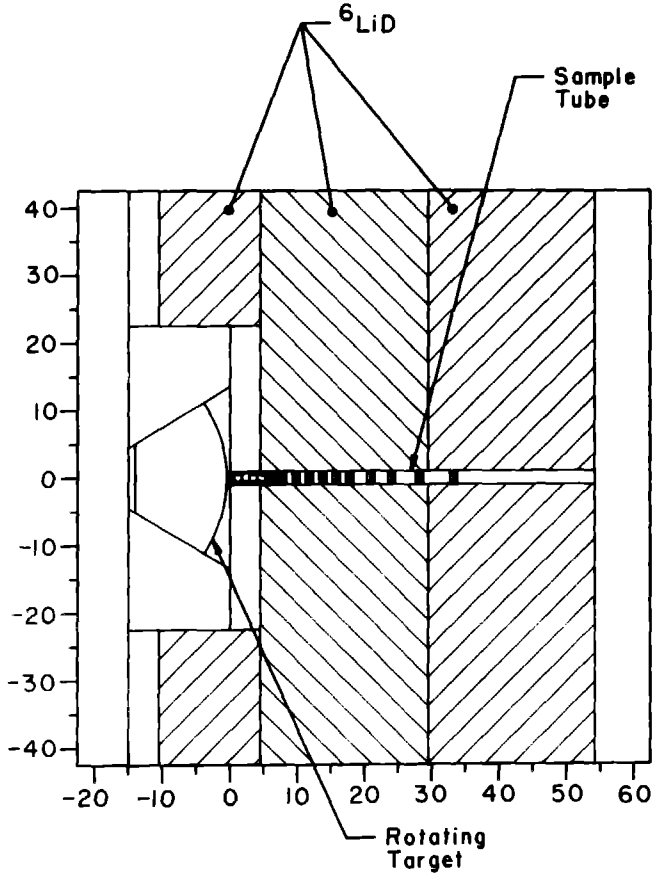
^{6}LiD
Sample Tube
40
30
20
10
0
-10
-20
-30
-40
-20
-10
0
10
20
30
40
50
60
Rotating Target

Fig. 2

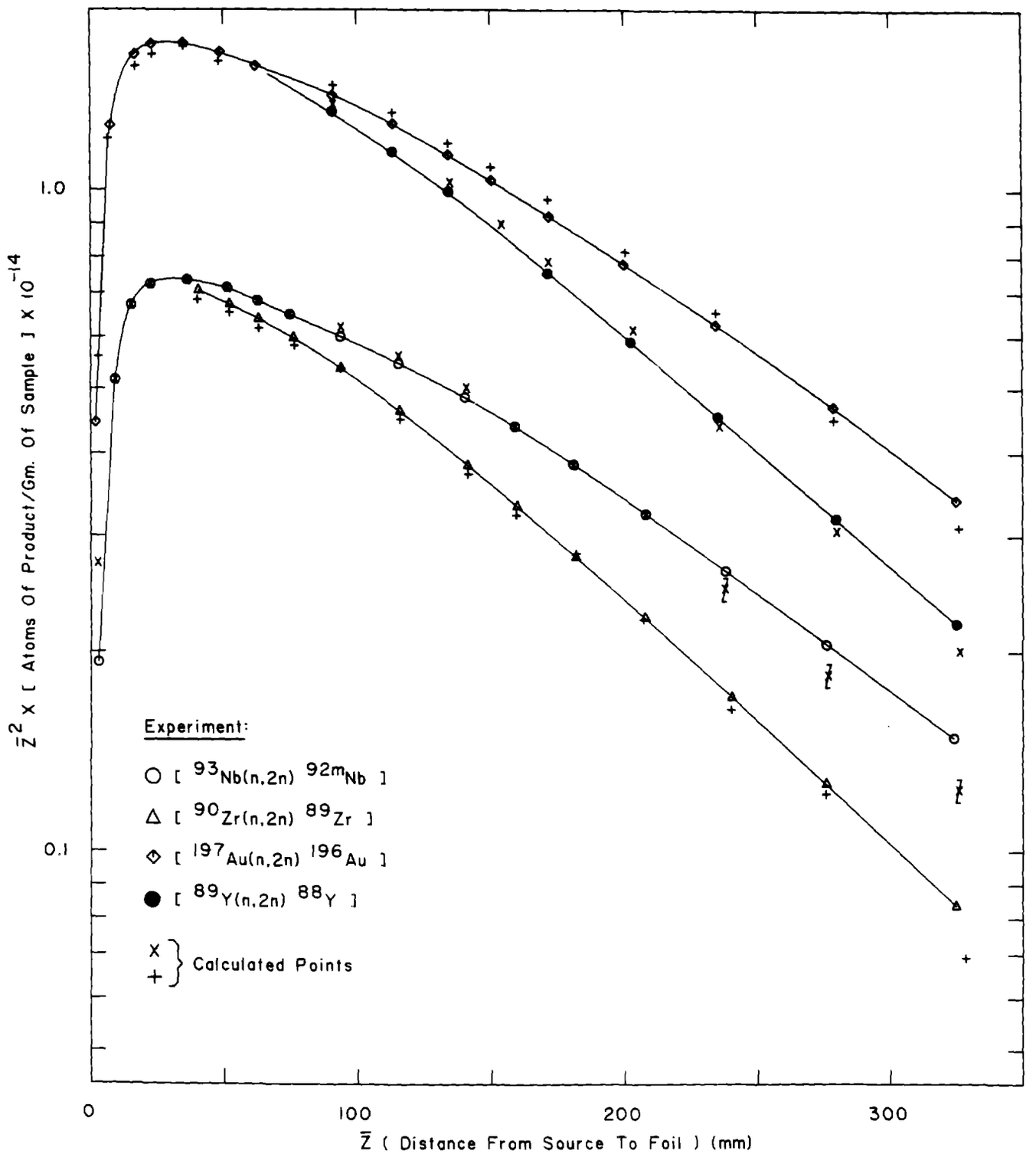
1.0
0.1
$\bar{Z}^2$ X [Atoms Of Product/Gm. Of Sample] X 10^{-14}
Experiment:
○ [^{93}Nb(n,2n) ^{92m}Nb]
△ [^{90}Zr(n,2n) ^{89}Zr]
◇ [^{197}Au(n,2n) ^{196}Au]
● [^{89}Y(n,2n) ^{88}Y]
X
+
Calculated Points
0
100
200
300
$\bar{Z}$ (Distance From Source To Foil) (mm)

Fig. 3

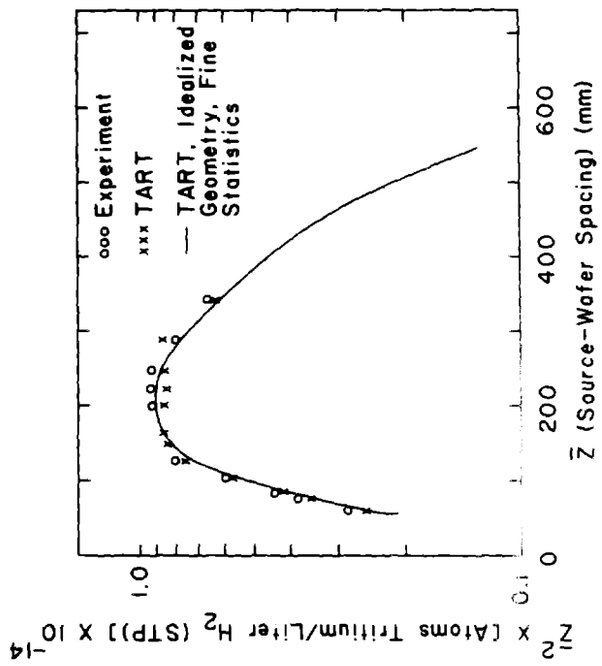
ooo Experiment
xxx TART
— TART, Idealized Geometry, Fine Statistics
1.0
0.1
0
200
400
600
$\bar{Z}$ (Source-Wafer Spacing) (mm)
$\bar{Z}^2$ x [Atoms Tritium/Liter H_2 (STP)] x 10^{-14}

Fig. 4

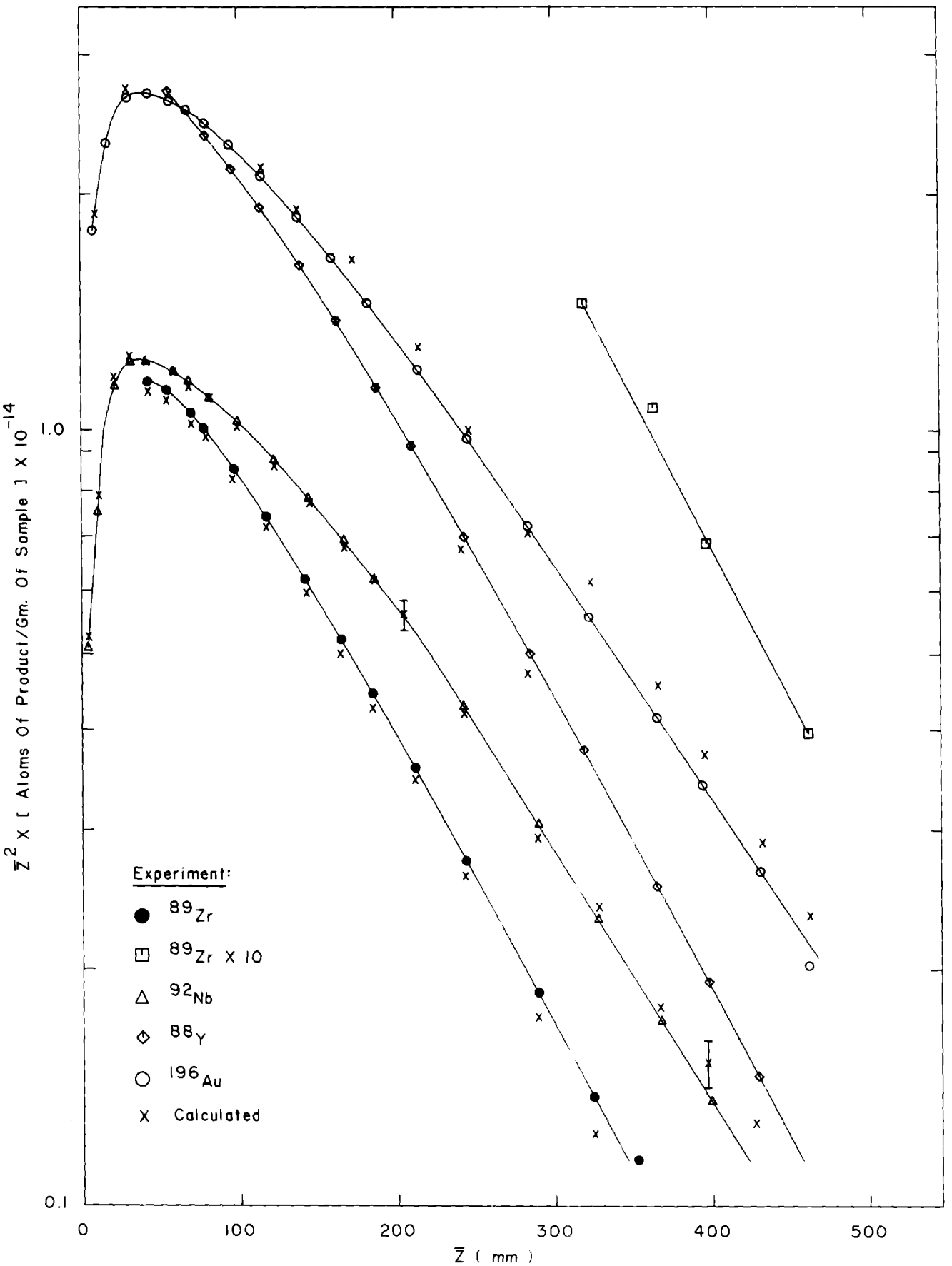
$\bar{Z}^2$ X [Atoms Of Product/Gm. Of Sample] X 10^{-14}
1.0
0.1
0
100
200
300
400
500
$\bar{Z}$ (mm)
Experiment:
^{89}Zr
^{89}Zr X 10
^{92}Nb
^{88}Y
^{196}Au
Calculated

Fig. 6

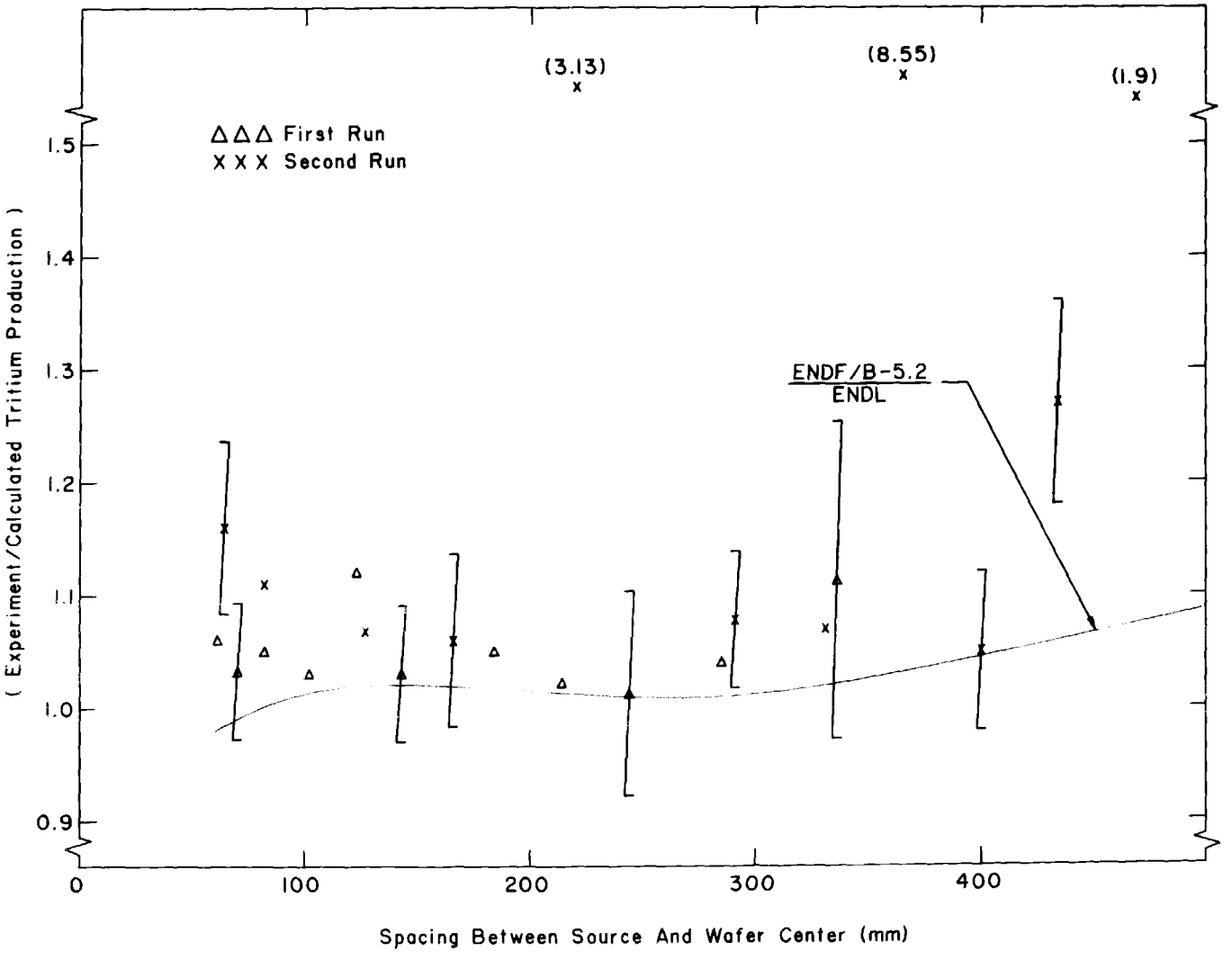
(3.13)
(8.55)
(1.9)
ΔΔΔ First Run
X X X Second Run
ENDF/B-5.2
ENDL
(Experiment/Calculated Tritium Production)
1.5
1.4
1.3
1.2
1.1
1.0
0.9
0
100
200
300
400
Spacing Between Source And Wafer Center (mm)

Fig. 7

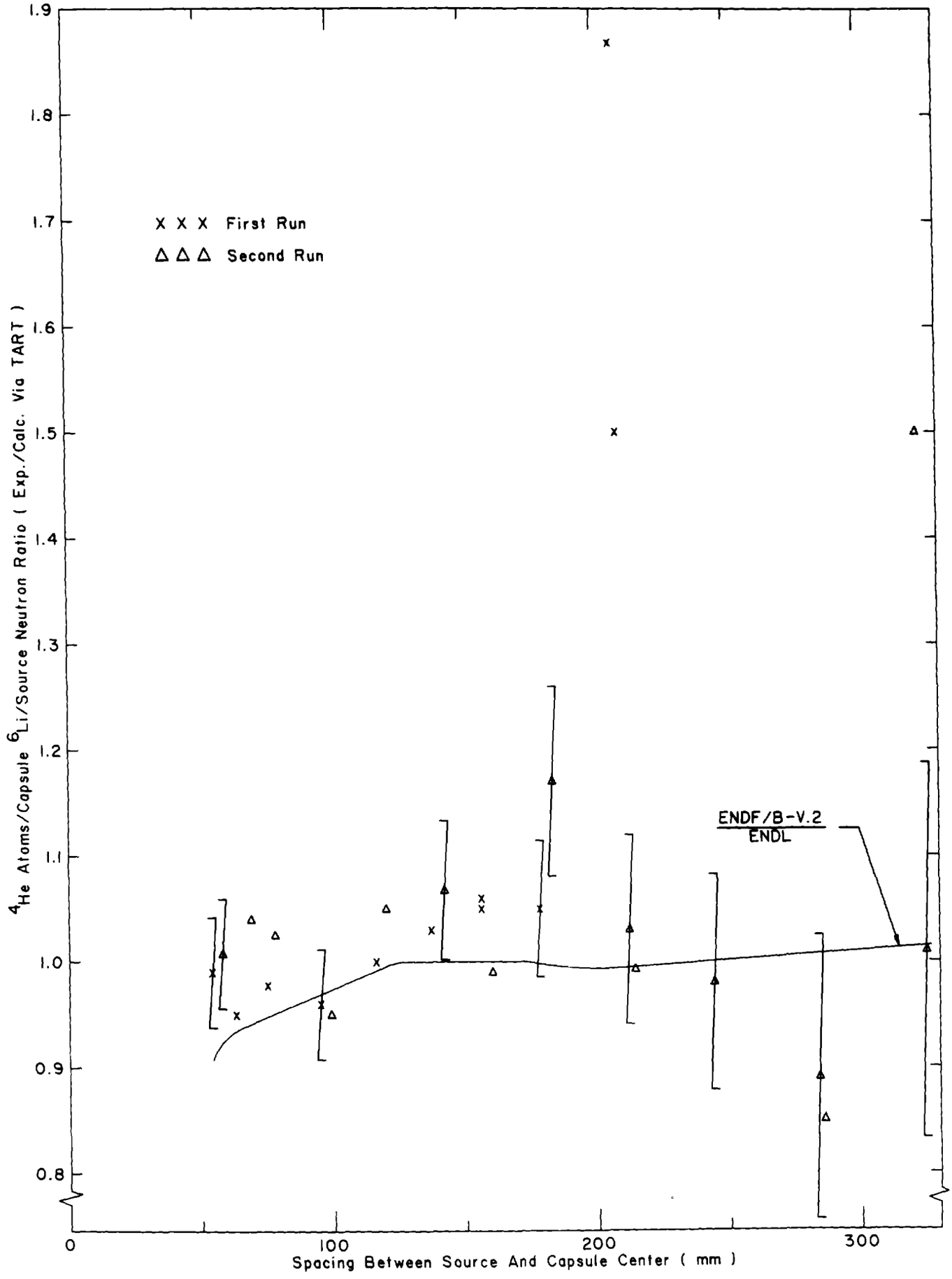
1.9
1.8
1.7
1.6
1.5
1.4
1.3
1.2
1.1
1.0
0.9
0.8
X X X First Run
Δ Δ Δ Second Run
ENDF/B-V.2
ENDL
^{4}He Atoms/Capsule ^{6}Li/Source Neutron Ratio (Exp./Calc. Via TART)
0
100
200
300
Spacing Between Source And Capsule Center (mm)

Fig. 8